



Determination of the time dependent magnetic field distribution in Pulsed-Power Systems

Y. Maron, R. Arad, G. Davara, L. Gregorian, Ya. Krasik, E. Kroupp,
M. Sarfaty, R. Shpitalnik, and A. Weingarten
Faculty of Physics
Weizmann Institute of Science
Rehovot, 76100, Israel

Abstract

Time-dependent measurements of the magnetic field distributions in diode, plasma opening switch, and Z-pinch plasmas, based on the observation of the Zeeman effect or of the ion acceleration, are reviewed. Relatively high spatial resolution is obtained by locally doping the plasma with the desired species. Besides information on the device properties, the measurements allowed for determining the plasma conductivity and for investigating the field penetration mechanism. Determination of the current density allowed the electron drift velocity to be known.

I. Introduction

The distribution of magnetic fields in the plasmas or in the non-neutral regions of pulsed power systems significantly affects the current flow, the resultant plasma heating, the plasma motion, and the thermal convection, and thus plays an important role in the overall operation of the devices. Therefore, development of nonintrusive methods for reliably observing the time dependent magnetic field distribution in such configurations, with satisfactory accuracy and spatial resolution, is of major importance. Here, we review measurements of the B-field distribution in Ion diode, Z-pinch, and Plasma Opening Switch (POS) experiments.

The methods used for measuring the magnetic field distributions are the observations of the Zeeman splitting of emission lines¹⁻⁴⁾ and observation of the ion acceleration due to the magnetic field gradients from the emission line Doppler shifts^{3,5)}. Together with the electron density determined independently, the latter yields the magnetic field gradient⁵⁾.

II. Local plasma doping

For studying the time dependent magnetic field penetration into a plasma, obtaining spatially resolved measurements of the magnetic field along the direction of penetration is a necessity. Since spectroscopic observations of spontaneous emission are integrated along the line of sight, the only way to achieve local measurements is by locally doping the plasma with the species that produces the line emission desired for the diagnostics. In doping the plasma it should be ascertained that the doped material is sufficiently low in density to cause no significant perturbations in the plasma properties, namely, the electron density and temperature, ionic composition, and the ion velocity distribution (this has been systematically examined in our experiments but will not be discussed in this report). The measurement spatial resolution is determined by doping the plasma in a region of the smallest size that allows for the required line intensity.

An additional advantage in employing plasma doping is that it allows for selecting lines of various species, suitable for the determination of the magnetic field under various conditions. For example, one should select heavy ions if the Zeeman splitting is to be

discriminated against the Doppler broadening, light ions if the line Doppler shifts are used to give the ion acceleration, lines from low-lying levels in order to minimize the Stark broadening, and lines from high-lying levels in order to reduce the opacity effect. The opacity can also be reduced by using a sufficiently low density for the doped material.

Various methods are used for the plasma doping. Material that contains the desired species can be deposited on electrodes in the devices. If plasma is formed over the electrode surface, particles originating in that material will be ejected into the plasma, and then ionize to various charge states. In the ion diode experiment¹⁾ the anode was coated with compounds of barium, which provided enough BaII in the surface-flashover-produced anode plasma. An additional advantage in using BaII in this experiment was that BaII propagated in the plasma relatively slowly and ionized into higher charge states within $\lesssim 0.1$ mm from the anode surface. Thus, we could obtain the magnetic field within 0.1 mm from the anode surface, enabling us to determine the value of the B-field that fully penetrates the $\simeq 2$ -mm-thick anode plasma.

In the 100-ns coaxial POS experiment^{2,3,5)}, material was deposited on the inner electrode (the anode) and was evaporated into the anode-cathode gap using a $\simeq 10$ GW/cm², 10 ns laser pulse focused on a spot $\simeq 200$ μ m in diameter. The POS current was applied about 3 μ s after the laser pulse allowing the doped species to propagate over most of the 2.5-cm anode-cathode gap. Here, barium was deposited on the anode for the observation of the Zeeman effect, and magnesium was used for the determination of the magnetic field by the ion-acceleration method.

In this POS experiment a 2D mapping of the magnetic field in the r, z plane was achieved. In the experiments, the doped column position was varied in the z direction over the plasma axial dimension. The spatial resolution in the axial (given by the doped-column width) and the radial (determined by the optical arrangement) were $\simeq 1$ and 0.02 cm, respectively. As yet, the field was measured at a single azimuth.

Another method to dop the plasma, developed in our 0.5 μ s POS experiment, is by injecting a narrow beam of gas into the anode-cathode gap through a hole in the cathode⁶⁾. The seeding arrangement consists of an ultrafast gas valve and a skimmer to collimate the beam. It allows for doping the plasma with various gaseous elements including noble gases. Another advantage is that it makes possible doping the plasma with higher-density neutral particles whose motion is unaffected by the magnetic field, which results in little Doppler broadening for the line. Also with this method a spatial resolution better than that obtained by the laser evaporation technique was achieved.

For the Z-pinch experiment no plasma doping was used. The line emission was observed parallel to the pinch axis with the optical arrangement designed to give spatial resolution of $\simeq 0.4$ and 2 mm in the radial the azimuthal directions, respectively⁴⁾. In a previous study⁷⁾ we found that during the implosion phase the lower-charge-state ions reside closer to the axis than the higher-charge-states ions. Based on these findings we performed axial observations of the imploding plasma, utilizing line emissions of various charge state ions at different times and radial locations.

III. Polarization spectroscopy

In the relatively low density plasmas the Zeeman splitting can mainly be obscured by Doppler broadening due to the ion motion under the magnetic field. Therefore, relatively heavy ions should be doped in order to minimize the ion velocities. In the diode measurements the use of BaII ions resulted in a well distinguished Zeeman splitting in the line

profile¹⁾. The observation of the Zeeman splitting and the use of repeated shots allowed an accuracy of $\simeq \pm 2\%$ for the magnetic field measurements to be achieved (this accuracy made possible the observation of the diamagnetic effect of the electron flow in the diode gap see below). In the POS measurements, however, the Zeeman splitting of the BaII line was comparable to the Doppler broadening. In these measurements, therefore, both spectral profiles of the σ and π line components had to be measured (the π -component profile is mainly affected by the Doppler broadening). The Zeeman splitting and Doppler broadening are then obtained self-consistently by comparing a calculation of the profiles of both components to the measured ones^{2,3)}.

In the higher density plasmas (the Z-pinch experiment), the line profile can also be affected by Stark broadening and opacity. Therefore, calculations⁸⁾ of line Stark broadening for the time and space varying electron densities were used to select lines with the smallest broadening. Also, collisional radiative calculations were used to obtain the atomic level populations, allowing for calculating the opacity effects and their influence on the line shape. In the measurements reported here for the Z-pinch experiment, the spectral profiles of the lines selected were dominated by Stark broadening, which was about twice the average Zeeman splitting of the various line components⁴⁾. Nevertheless, the use of polarization spectroscopy as described in the above, allowed for determining the magnetic field with a reasonably good accuracy. This was made possible by using sufficiently intense lines and achieving a high accuracy for the line profile measurements.

The diagnostic systems for the various experiments are described in Refs. 1-5. In brief, the systems allow for measuring the time dependent spectral profiles of two emission lines, or the profiles of the σ and π components of a single line, in a single discharge.

IV. Results

A) Magnetically insulated ion diode

For the diode experiment we used a planar magnetically insulated diode¹⁾. Light was collected from the anode plasma parallel to the lines of the externally applied magnetic field. The measurements were integrated along the anode length and the spatial resolution in the gap direction was < 0.1 mm.

An example of the measured magnetic field in the plasma is shown in Fig. 1. To within the uncertainties, the magnetic field in the anode plasma at early times equals the applied magnetic field ($7.6 \pm 10\%$ kG). The magnetic field then rises by $\simeq 0.8$ kG during the pulse, then drops to about the applied field when the diode current I is zero ($t \simeq 150$ ns), followed by a decrease below the applied field when $I < 0$. The magnetic field rises again above the applied field when I rises ($t \geq 250$ ns). This demonstrates the diamagnetic effects of the electron flow in the diode acceleration gap.

The rise in the magnetic field on the anode side due to the electron flow within the first 100 ns of the pulse was found to be much larger than that obtained from a one-dimensional Brillouin-flow model calculation. However, it was consistent with estimates⁹⁾ based on the measured ion current density and on the electric field distribution across the diode acceleration gap observed¹⁰⁾ for a similar diode configuration. Those observations¹⁰⁾ showed significant electron flow close to the anode plasma, beyond the calculated electron-sheath region, which should enhance the diamagnetic effect on the anode side.

The penetration into the anode plasma of the diamagnetic signal due to the electron flow in the gap was calculated using the magnetic diffusion equation in which the plasma

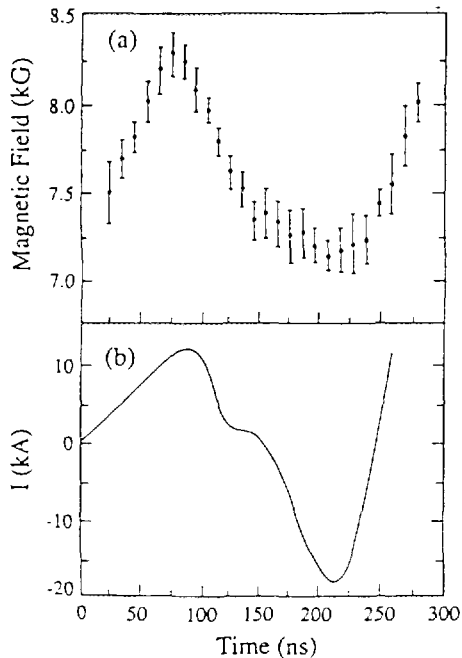


Fig. 1(a) Magnetic field as a function of time, within 0.1 mm from the anode surface of a magnetically insulated ion diode, observed using the BaII 6142 Å line. The data points are averaged over $N=11$ identical discharges. The error bars shown for each time are the standard deviations divided by $\sqrt{N-1}$. Besides these error bars shown there is an uncertainty of $\pm 6\%$ in the absolute value of the observed magnetic field; (b) The diode total-current waveform.

conductivity is a parameter. The calculated field penetration was found to be consistent with a plasma conductivity $10\times$ lower than the Spitzer conductivity, known from an experimental determination of the electron temperature and the ionic composition of the plasma¹¹). This anomalous conductivity and the observed magnetic field were also found to be in agreement with the observed rate of the plasma expansion against the magnetic field and the uniformity of the electron temperature in the plasma¹¹). The latter was examined using an estimate of the thermal convection based on the measured magnetic field^{11,12}). Furthermore, together with the pressure-driven current in the plasma, this conductivity yielded a reasonable Ohmic heating rate for the plasma electrons. In addition, the effect of the magnetic field in the plasma on the flow of various ionic species, and thus its influence on the composition of the extracted ion beam, could also be studied¹³).

B) Plasma Opening Switch

Our POS is coaxial with the inner electrode (the anode) charged positively. The inner and outer electrode radii are 2.5 and 5 cm, respectively, and the peak current is $\simeq 135$ kA with quarter period of 90 ns. The plasma is produced by a gaseous plasma source, which is mounted inside the anode and injects the plasma radially outward. The plasma axial dimension is $\simeq 4$ cm. For the Zeeman-splitting observations, two spectrometers were employed to measure the line σ and π components simultaneously in a single discharge.

Results on the magnetic field penetration velocity and the time dependent 2-D structure of the magnetic field are given elsewhere^{2,3}). Here, we only mention a few findings. Figure 2 shows the axial B -field distributions at $t=20, 30$, and 50 ns after the beginning of the current at the generator side edge of the plasma, obtained from the Zeeman splitting of a BaII line. The magnetic field was observed to penetrate into the plasma at a velocity of $\simeq 10^8$ cm/sec, three orders of magnitude higher than the diffusion velocity, and higher than the Alfvén velocity. The high penetration velocity and the sharp gradient of the magnetic field in the axial direction indicate penetration in the form of a shock. At $t=30$ ns the field also appears at the load side of the plasma, while it is still close to zero at $z \simeq 0.5$ cm. At

$t = 50$ ns, field is present over the entire plasma. At that time it is found that most of the current flows at the load-side edge of the plasma and between the plasma and the load (see below).

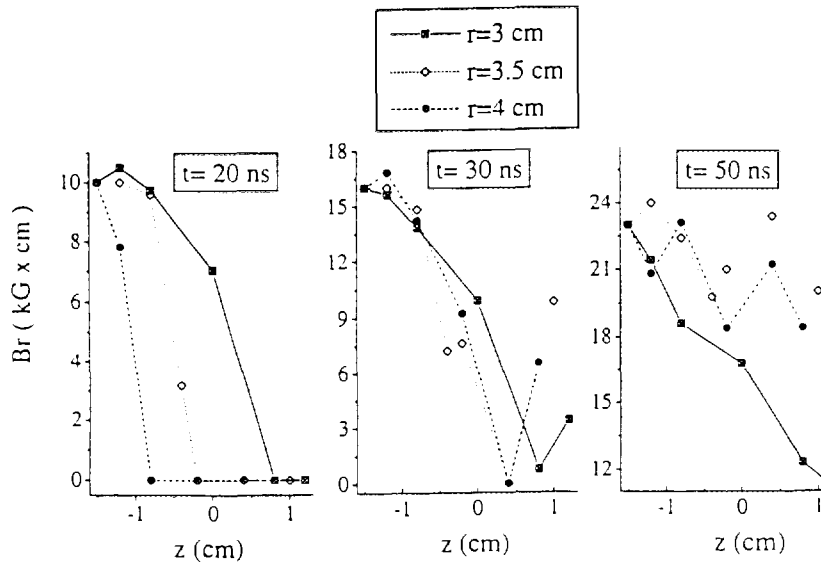


Fig. 2 The magnetic field (multiplied by the radius) as a function of the axial distance in the POS for three radial positions $r=3$, 3.5, and 4 cm at (a) $t=20$ ns, (b) $t=30$ ns, and (c) $t=50$ ns after the start of the current pulse. $z=0$ is the injected plasma axial center with the generator side denoted by a negative z .

The evolution of the magnetic field distribution was calculated using a model based on the Hall effect^{14,15}). In the model we used our measured electron density distribution and assumed fast penetration along the POS electrodes³). The results were found to be in good agreement with the data given in the above.

Using the ion-acceleration method, the velocity distributions for various-charge-state ions were observed^{2,5}). The magnetic field axial distributions for various times, obtained by measuring the Doppler shifts of line emission of MgII doped in the plasma, are shown in Fig. 3. Here, the magnetic field could also be measured at the load-side edge of the plasma, showing a relatively high current density in this region. This is expected to cause plasma acceleration towards the load, as supported by charge collection measurements. Also, the difference between B observed in the load-side edge of the plasma and that measured at the load shows a current loss between the switch plasma and the short-current load.

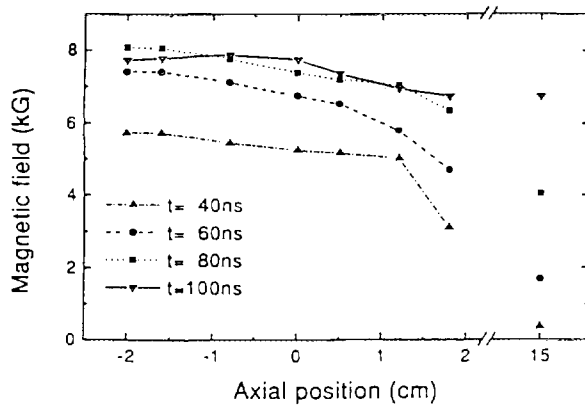


Fig. 3 Axial magnetic field distributions for several times at $r=3.2$ cm (0.7 cm from the anode surface) obtained from axial time-dependent local velocities of MgII doped in the plasma. In obtaining B , we used an electron density 1.3×10^{14} cm^{-3} , determined from the observed particle ionization times. The data points are connected by straight lines. The points at $z=15$ cm give the magnetic field measured by the Rogowski coil near the shorted load.

C) Z-pinch experiment

In the Z-pinch experiment⁴⁾ we employ a gas-puff device for the injection of a hollow cylinder of gas (CO₂ or, argon). The anode-cathode gap is 1.35 cm, and the diameters of both anode and cathode are 4 cm. The plasma pinches at $\simeq 620$ ns after the start of the current pulse, when the current is $\simeq 220$ kA.

The dominance of the Stark effect over the line Zeeman splitting as mentioned above, required the observation of the π and σ line components. For each polarization we performed at least 20 discharges, thus obtaining an uncertainty of $\simeq \pm 2\%$ in the FWHM of the averaged profile. The experimental data points were then fitted to a Lorentzian. The spectral line profiles were calculated for each polarization based on the Zeeman splitting and Stark broadening as input parameters. Comparison to the measured profiles yielded the magnetic field at each radius and time, with an accuracy of 15-20%. Detailed description of the line profiles observed and a discussion on the accuracy is given in a separate report⁴⁾. Here we only present the radial distribution of the magnetic field obtained for two times during the implosion, as shown in Fig. 4. The fitting curves presented are obtained from solutions of a 1-D magnetic diffusion equation the boundary conditions of which (namely, the outer plasma radius and the magnetic field at this radius) are determined experimentally⁴⁾, and in which the plasma conductivity is a parameter. The best-fit curves given in Fig. 4, yield plasma conductivity that is close to the Spitzer value. Also given in Fig. 4 are the values of the boundary field B_o , obtained using the total discharge current in the plasma measured by a Rogowski loop. The good agreement between B_o and the spectroscopically determined magnetic field at the plasma outer radius indicate that the entire current flows through the plasma. The distributions given in Fig. 4 also show that the B field penetration depth is about half of the plasma shell thickness.

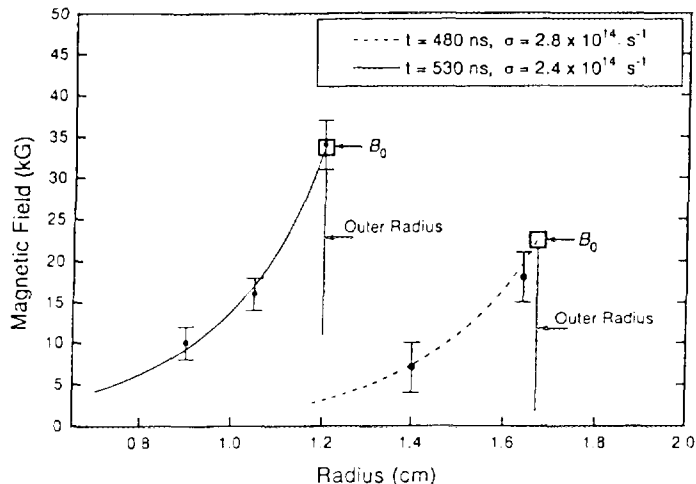


Fig. 4 The magnetic field distribution in the plasma at $t = 480$ and 530 ns (the pinch occurs at $\simeq 620$ ns). The curves are best-fit solutions of the magnetic field diffusion equation using plasma conductivity σ as indicated. The $1/e$ decrease of the magnetic field occurs at distances of 0.24 and 0.22 cm from the plasma outer radius for $t = 480$ and $t = 530$ ns, respectively. B_o is the field calculated using the total discharge current measured by a Rogowski loop.

Using these results we calculated the $J \times B$ forces across the plasma shell and compared it to the radial acceleration of the various charge-state ions obtained from the line-emission Doppler shifts. This comparison yielded the temporal and radial distributions of the contributions of the magnetic field pressure and the thermal pressure to the radial acceleration.

Summary

The magnetic field distribution can be measured in various pulsed power systems with satisfactory accuracy and spatial resolution. In principle, methods based on laser spectroscopy can also be utilized. For example, the use of laser-induced two-photon processes with the appropriate geometry is expected to allow for measurements of smaller magnetic fields with an improved spatial resolution in all directions¹⁶). Observation of the magnetic field in higher power z-pinchs may be possible using VUV line emission.

References

1. Y. Maron, E. Sarid, E. Nahshoni, and O. Zahavi, *Phys. Rev.* **A39**, 5856 (1989).
2. M. Sarfaty, R. Shpitalnik, R. Arad, A. Weingarten, Ya.E. Krasik, A. Fruchtman, and Y. Maron, *Phys. Plasmas* **2**(6), 2583 (1995).
3. R. Shpitalnik, A. Weingarten, K. Gomberoff, Ya. Krasik, and Y. Maron, Observations of fast Magnetic Field Penetration in a Plasma Opening Switch, WIS Report, WIS/96/15/Mar.-PH, 11th Int. Conference in High Particle Beams, Prague, Czech Rep., June 10-14, 1996, to be published.
4. G. Davara, L. Gregorian, E. Kroupp, and Y. Maron, 11th Int. Conference in High Particle Beams, Prague, Czech Rep., June 10-14, 1996, WIS-96/16/Feb.-PH Report, to be published; L. Gregorian et al., these proceedings.
5. M. Sarfaty, Y. Maron, Ya. E. Krasik, A. Weingarten, R. Arad, R. Shpitalnik, A. Fruchtman, and Y. Maron, *Phys. Plasmas* **2**(6), 2122 (1995).
6. R. Arad, Ya. Krasik, L. Ding, and Y. Maron, 11th Int. Conference in High Particle Beams, Prague, Czech Rep., June 10-14, 1996, to be published.
7. M.E. Foord, Y. Maron, G. Davara, L. Gregorian, and A. Fisher, *Phys. Rev. Lett.* **72**, 3827 (1994).
8. S. Alexiou, *Phys. Rev. Lett.* **75**, 3406 (1995); S. Alexiou and Y. Maron, *J. Quantitative Spectroscopy and Radiative Transfer*, Vol. 53, pp 109-124 (1995); S. Alexiou and Yu. Ralchenko, *Phys. Rev.* **A49**, 3086 (1994).
9. C.W. Mendel, Jr. and J.P. Quintenz, *Comments Plasma Phys. Controlled Fusion* **8**, 43 (1983).
10. Y. Maron, M.D. Coleman, D.A. Hammer, and H.S. Peng, *Phys. Rev.* **36**, 2818 (1987).
11. Y. Maron, M. Sarfaty, L. Perelmutter, O. Zahavi, M.E. Foord and E. Sarid, Electron temperature and heating processes in a dynamic plasma of a high power diode, *Phys. Rev.* **A40**, 3240 (1989).
12. S.I. Braginskii, in *Review of Plasma Physics*, edited by M.A. Leontovich, Vol. 1, p.205., (1965).
13. Y. Maron, L. Perelmutter, E. Sarid, M.E. Foord, and M. Sarfaty, *Phys. Rev.* **A41**, 1074 (1990).
14. A.S. Kingsep, L.I. Rudakov, and K.V. Chukbar, *Sov. Phys. Dokl.* **27**, 140 (1982); A.S. Kingsep, K.V. Chukbar, and V.V. Yankov, in *Review of Plasma Physics*, edited by B.B. Kadomstev (Consultants Bureau, New York, 1990), Vol. 16, p.243.
15. A. Fruchtman, *Phys. Rev.* **A45**, 3938 (1992); A. Fruchtman, and K. Gomberoff, *Phys. Fluids* **B5**, 2371 (1993).
16. Y. Maron and C. Litwin, *J. Appl. Phys.* **54** 2086 (1983).